THE AMERICAN SOCIETY OF MECHANICAL ENGINEERS
345 E. 47th St., New York, N.Y. 10017

96-GT-160

CALCULATION OF TRANSITION IN ADVERSE PRESSURE GRADIENT FLOW BY CONDITIONED EQUATIONS.

J. Steelant and E. Dick

Department of Mechanical and Thermal Engineering
Universiteit Gent
Sint Pietersnieuwstraat 41, 9000 Gent,
Belgium.

ABSTRACT

Conditionally averaged Navier-Stokes equations are used to describe transitional flow in adverse pressure gradient combined with a transport equation for the intermittency factor γ. A transport equation developped in earlier work has been modified to eliminate the use of a distance along a streamline. An extension of the correlations is proposed to determine the spot growth parameter in adverse pressure gradient. This approach is verified against flows over a flat plate with an elliptical leading edge.

INTRODUCTION

In turbomachinery flow, the extent of the transition zone relative to the blade chord, can be very large. This zone is characterized by the presence of turbulent spots in a pseudo-laminar flow. The spots grow in size when convected downstream at a rate which is primarily dependent on the mean flow turbulence level and the pressure gradient. The evolution of the spot growth can he quantified by the intermittency factor γ which gives the relative fraction of time the flow is turhulent during the transitional phase. Transition models based on conditional averages calculate the state of hoth the turhulent spot and the laminar flow. To define the global result, a weighting, based on the intermittency factor γ, of the turbulent and the laminar conditioned average is made. If no interaction is assumed at the interfaces of the turbulent spot with the laminar flow, then the turbulent and laminar average can be calculated separately. These methods are referred to as linear combination models (e.g. Gostelow et *al.* (1994a)).

This assumption is acceptable for global parameters in zero and favourable pressure gradient flow. However, in an adverse pressure gradient, the interaction at the interface of the spot cannot be neglected. Due to the entrainment of the turbulent spot, the laminar layer remains attached to the wall. In linear combination models, the laminar flow calculation will predict separation. By conditional averaging the Navier-Stokes equations, interaction terms arise which model the entrainment and prevent the laminar state from separating. The obtained averages are then linearly combined by use of the intermittency factor γ. This factor is determined by a transport equation where the spot growth dependency on the pressure gradient and the turbulence level has been taken into account.

NOMENCLATURE

C_f	skin friction, $\tau_w/(\rho U_e^2/2)$.
k	turbulence kinetic energy.
K	acceleration parameter, $\frac{\nu}{U_e^2}\frac{dU_e}{dx}$.
Re_x	Reynolds number, $U_e x/\nu$.
Re_θ	momentum thickness Reynolds number, $U_e\theta/\nu$
Tu	turbulence intensity, $100\sqrt{k}/U_e(\%)$.
$\overline{u}$	global time averaged velocity.
$\overline{u}_t$	averaged velocity during turhulent state.
$\overline{u}_l$	averaged velocity during laminar state.
u', v'	fluctuating velocity components.
γ	intermittency factor.
ϵ	turbulence dissipation.
μ	dynamic viscosity.
ρ	density.
θ	momentum thickness.

Presented at the International Gas Turbine and Aeroengine Congress & Exhibition
Birmingham, UK — June 10-13, 1996

Sub- and superscripts

e	edge of boundary layer.
l	laminar state.
t	turbulent state.
s	start of transition ($\gamma = 1\%$)
$\tilde{}$	conditioned Favre-average.
$\bar{}$	conditioned Reynolds-average.

CONDITIONED FLOW EQUATIONS

Conditionally averaged Navier-Stokes equations (Steelant and Dick, 1995) lead both for the laminar and turbulent phases in an intermittent flow to a set of equations for mass, momentum and energy. These conditioned equations differ from the original Navier-Stokes equations by the presence of source terms which are function of the intermittency factor γ. The source terms model the interaction between both phases. The conditionally averaged laminar and turbulent equations can be written in vector form as:

$$\frac{\partial \overline{U}_l}{\partial t} + \frac{\partial \overline{F}_l}{\partial x} + \frac{\partial \overline{G}_l}{\partial y} = \frac{\partial \overline{F_v}_l}{\partial x} + \frac{\partial \overline{G_v}_l}{\partial y} + S_l^\gamma, \quad (1)$$

$$\frac{\partial \overline{U}_t}{\partial t} + \frac{\partial \overline{F}_t}{\partial x} + \frac{\partial \overline{G}_t}{\partial y} = \frac{\partial \overline{F_v}_t}{\partial x} + \frac{\partial \overline{G_v}_t}{\partial y} + S_t^\gamma, \quad (2)$$

with

$$\overline{U}_l = \left\{ \overline{\rho}_l, \overline{\rho}_l \tilde{u}_l, \overline{\rho}_l \tilde{v}_l, \overline{\rho}_l \tilde{E}_l \right\},$$

$$\overline{U}_t = \left\{ \overline{\rho}_t, \overline{\rho}_t \tilde{u}_t, \overline{\rho}_t \tilde{v}_t, \overline{\rho}_t \tilde{E}_t, \overline{\rho}_t \tilde{k}_t, \overline{\rho}_t \tilde{\epsilon}_t \right\}.$$

The convective and diffusive terms in x- and y-direction are denoted respectively by F, G and F_v, G_v. The set of laminar equations (1) differs from the classical Navier-Stokes equations by the source terms:

$$S_l^{\gamma^T} = \frac{1}{2(1-\gamma)} \left\{ S_\rho^\gamma; S_{\rho u}^\gamma; S_{\rho v}^\gamma; S_{\rho E}^\gamma \right\}.$$

The set of turbulent equations (2) consists besides of the four Navier-Stokes equations also of the turbulent k-ϵ equations. The source terms are

$$S_t^{\gamma^T} = \left\{ \frac{1}{2\gamma} S_\rho^\gamma; \frac{1}{2\gamma} S_{\rho u}^\gamma; \frac{1}{2\gamma} S_{\rho v}^\gamma; \frac{1}{2\gamma} S_{\rho E}^\gamma; S_{\rho k}; S_{\rho \epsilon} \right\}.$$

Both sets of equations (1) and (2) have to be solved simultaneously in each point of the flow field. Global quantities are obtained by weighting the laminar and turbulent quantities. The interaction terms arising in the laminar and turbulent Navier-Stokes equations are:

$$S_\rho^\gamma = (\overline{\rho}_l - \overline{\rho}_t)\frac{\partial \gamma}{\partial t} + (\overline{\rho}_l \tilde{u}_l - \overline{\rho}_t \tilde{u}_t)\frac{\partial \gamma}{\partial x} + (\overline{\rho}_l \tilde{v}_l - \overline{\rho}_t \tilde{v}_t)\frac{\partial \gamma}{\partial y},$$

$$S_{\rho u}^\gamma = (\overline{\rho}_l \tilde{u}_l - \overline{\rho}_t \tilde{u}_t)\frac{\partial \gamma}{\partial t} + (\overline{\rho}_l \tilde{u}_l \tilde{u}_l - \overline{\rho}_t \tilde{u}_t \tilde{u}_t)\frac{\partial \gamma}{\partial x}$$
$$+ (\overline{\rho}_l \tilde{u}_l \tilde{v}_l - \overline{\rho}_t \tilde{u}_t \tilde{v}_t)\frac{\partial \gamma}{\partial y} + (\overline{p}_l - \overline{p}_t - \frac{2}{3}\overline{\rho}_t \tilde{k}_t)\frac{\partial \gamma}{\partial x}$$
$$- \left[\overline{\mu}_l \tilde{S}_{lxx} - (\overline{\mu}_t + \mu_e)\tilde{S}_{txx}\right]\frac{\partial \gamma}{\partial x}$$
$$- \left[\overline{\mu}_l \tilde{S}_{lxy} - (\overline{\mu}_t + \mu_e)\tilde{S}_{txy}\right]\frac{\partial \gamma}{\partial y},$$

$$S_{\rho v}^\gamma = (\overline{\rho}_l \tilde{v}_l - \overline{\rho}_t \tilde{v}_t)\frac{\partial \gamma}{\partial t} + (\overline{\rho}_l \tilde{v}_l \tilde{u}_l - \overline{\rho}_t \tilde{v}_t \tilde{u}_t)\frac{\partial \gamma}{\partial x}$$
$$+ (\overline{\rho}_l \tilde{v}_l \tilde{v}_l - \overline{\rho}_t \tilde{v}_t \tilde{v}_t)\frac{\partial \gamma}{\partial y} + (\overline{p}_l - \overline{p}_t - \frac{2}{3}\overline{\rho}_t \tilde{k}_t)\frac{\partial \gamma}{\partial y}$$
$$- \left[\overline{\mu}_l \tilde{S}_{lyx} - (\overline{\mu}_t + \mu_e)\tilde{S}_{tyx}\right]\frac{\partial \gamma}{\partial x}$$
$$- \left[\overline{\mu}_l \tilde{S}_{lyy} - (\overline{\mu}_t + \mu_e)\tilde{S}_{tyy}\right]\frac{\partial \gamma}{\partial y},$$

$$S_{\rho E}^\gamma = (\overline{\rho}_l \tilde{E}_l - \overline{\rho}_t \tilde{E}_t)\frac{\partial \gamma}{\partial t}$$
$$+ (\overline{\rho}_l \tilde{H}_l \tilde{u}_l - \overline{\rho}_t \tilde{H}_t \tilde{u}_t)\frac{\partial \gamma}{\partial x}$$
$$+ (\overline{\rho}_l \tilde{H}_l \tilde{v}_l - \overline{\rho}_t \tilde{H}_t \tilde{v}_t)\frac{\partial \gamma}{\partial y}$$
$$- \left[\overline{\tau}_{lxx}\tilde{u}_l + \overline{\tau}_{lxy}\tilde{v}_l - \overline{\tau}^{tot}_{txx}\tilde{u}_t - \overline{\tau}^{tot}_{txy}\tilde{v}_t\right]\frac{\partial \gamma}{\partial x}$$
$$- \left[\overline{\tau}_{lxy}\tilde{u}_l + \overline{\tau}_{lyy}\tilde{v}_l - \overline{\tau}^{tot}_{txy}\tilde{u}_t - \overline{\tau}^{tot}_{tyy}\tilde{v}_t\right]\frac{\partial \gamma}{\partial y}$$
$$+ \left[\overline{q}_{lx} - \overline{q}^{tot}_{tx}\right]\frac{\partial \gamma}{\partial x} + \left[\overline{q}_{ly} - \overline{q}^{tot}_{ty}\right]\frac{\partial \gamma}{\partial y}.$$

The mean total energy $\tilde{E}_t$ and mean total enthalpy $\tilde{H}_t$ during the turbulent phase are given by

$$\tilde{E}_t = \tilde{e}_t + \frac{1}{2}(\tilde{u}_t^2 + \tilde{v}_t^2) + \tilde{k}_t,$$

$$\tilde{H}_t = \tilde{E}_t + \frac{\overline{p}_t}{\overline{\rho}_t} + \frac{2}{3}\tilde{k}_t,$$

where $\tilde{e}_t$ is the mean internal energy. $\overline{\tau}^{tot}_{ti,j}$ are stress components formed by the sum of the Reynolds stress components and the mean molecular stress components during the turbulent phase. In the same way $\overline{q}^{tot}_{ti}$ are total heat flux components during the turbulent phase. The turbulence is modelled by the classical (low Reynolds number) k- and ϵ-equations, but written for the turbulent conditioned averaged values. Due to the good representations for zero (ZPG), favourable (FPG) and adverse (APG) pressure gradient flow, the Yang-Shih variant (Yang and Shib, 1993) has been chosen as low-Reynolds turbulence model.

In the sequel we study only steady flows. So all equations can be simplified by deleting the time derivative terms.

INTERMITTENCY MODELLING

To calculate the intermittency factor γ, a transport equation has been derived by Steelant and Dick (1995) which takes into account the distributed breakdown near the onset of transition:

$$\overline{\rho}\,\tilde{u}\frac{\partial \gamma}{\partial x} + \overline{\rho}\,\tilde{v}\frac{\partial \gamma}{\partial y} = (1-\gamma)\overline{\rho}\,\beta\sqrt{\tilde{u}^2+\tilde{v}^2}, \quad (3)$$

where β is a function of $s, \widehat{n\sigma}, K, Tu$, with s the distance to the point of transition along a streamline, $\widehat{n\sigma}$ the spot growth parameter, K the pressure gradient parameter and Tu the turbulence intensity in the free stream. The β-function was constructed for ZPG- and FPG-flows. In this work we extend the β-function to APG flows. Further we eliminate the dependence on the streamwise distance s, since this distance is difficult to define. The β-function can be written as (Steelant and Dick, 1995):

$$\beta = 2f'(s)f(s). \quad (4)$$

The function $f(s)$ can easily be determined in the case of concentrated breakdown:

$$f(s) = \sqrt{-\ln(1-\gamma)} = \sqrt{\widehat{n\sigma}}\frac{U_\infty}{\nu}s.$$

Equation (4) results then in:

$$\beta = 2f_\gamma \widehat{n\sigma}(K,Tu)\frac{U_\infty^2}{\nu^2}\sqrt{-\ln(1-\gamma)}.$$

with $f_\gamma = 1$. This equation for β does not contain s anymore.

Distibuted breakdown is modelled here by lowering the value of f_γ in the beginning of transition:

$$\begin{cases} \gamma < 0.45: & 1-\exp\left[-1.735\tan(5.45\gamma - .95375) - 2.2\right] \\ \gamma > 0.45: & 1 \end{cases}$$

The correlation for $\widehat{n\sigma}$ is extended to adverse pressure gradients ($K < 0$) by using the experimental data of Gostelow *et al.* (1991). In figure 1, the normalised spot growth parameter is given for different acceleration parameters K and turbulence levels. For favourable pressure gradients, the data were based on the experiments of Blair (1992). The correlations, shown in fig. 1, are:

$$\frac{\widehat{n\sigma}}{\widehat{n\sigma}_o} = \begin{cases} (474Tu^{-2.9})\left[1-\exp(2\times 10^6 K)\right] & K<0 \\ 10^{-3227K^{0.5985}} & K>0, \end{cases}$$

where $\widehat{n\sigma}_0$ is the value for $K = 0$. For ZPG- and FPG-flows, the present correlations for $\widehat{n\sigma}$ and f_γ reproduce the results of the previous paper. In bypass transition, the parameter $\widehat{n\sigma}_o$ and the point of transition,defined as the point where $\gamma = 1\%$, have been correlated by Mayle (1991) based on intermittency measurements for zero pressure gradient flow (ZPG) on flat plates as

$$\widehat{n\sigma}_o = 1.25\,10^{-11}Tu^{\frac{7}{4}}, \quad (5)$$

$$Re_{\theta_s} = 420\,Tu^{-.69}, \quad (6)$$

where Tu is the turbulence level at the leading edge. The expression (6) is also valid for pressure gradient flow under the condition that the turbulence level is sufficiently high (Mayle, 1991).

In order to avoid singularities in the calculations, the minimum and maximum value of γ are set to 0.01 and 0.99. These limits are normally taken as start and end of transition in experiments. Prior to the start of transition, determined from (6), γ is set equal to 0.01. The starting line is normal to the wall. Equation (3) then gives the evolution of the intermittency. The mechanism to let grow γ from 0.01 to 0.99 is mainly governed by the source term β. Equation (3) results in an almost constant distribution for γ normal to the wall, due to the absence of a diffusive term. Physically this is not

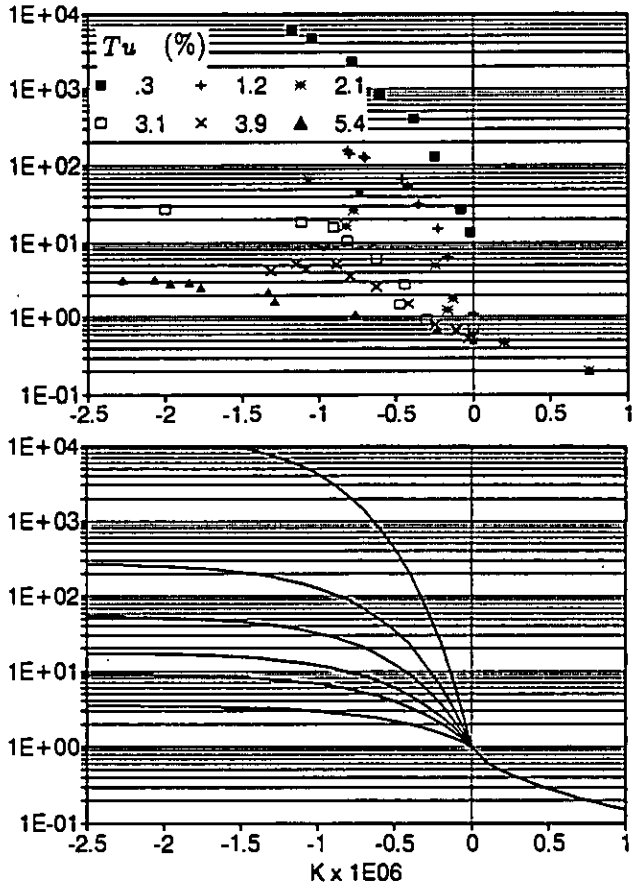

Figure 1: Normalised spot growth parameter: experiments (top) and correlations (bottom).

correct; γ should attain 1 in the free stream. We did not study yet the modelling of the γ-distribution normal to the wall since not enough experimental data on γ-profiles are yet availahle.

RESULTS

The above equations have been used to calculate intermittent flows on an adiabatic flat plate for a zero pressure gradient (ZPG) and adverse pressure gradient (APG). The equations are solved in their steady state form by a relaxation procedure. A vertex-centered finite volume discretization combined with an upwind TVD formulation is used. Full details of the numerical method are given by Steelant and Dick (1994).

The considered test cases are described extensively in Gostelow *et al.* (1991, 1994b). The flat plate has a length of 1500mm and a thickness of 24.5mm. The upper side of the flat plate has an elliptical shaped leading edge in order to prevent separation bubhles. The discretization of the geometry has heen done using a C-mesh with 147 points in normal and 257 points in tangential direction (fig. 2). In front of the plate, symmetry conditions have heen applied. No-slip conditions and an adiabatic boundary condition have heen used on the flat plate.

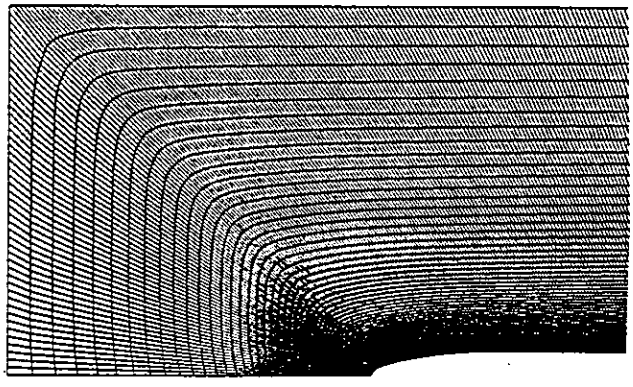

Figure 2: C-mesh for the flat plate.

The specifications of the different test cases are given in the table 1 where U_∞ stand for the velocity upstream of the leading edge, Tu_{le} is the turhulence level at the L.E., $\Delta x = x_{grid} - x_{le}$ is the relative position of the turbulence generating grid versus the L.E. and $\overline{K}$ is the mean acceleration parameter during the transition zone.

Case	U_∞	Tu_{le}	Δx	$\overline{K} \times 10^6$
SUG5K0	7.38	3.9	1.2	0.
SUG5K6	15.28	3.9	1.2	−0.9
SUG3K6	15.9	3.1	1.2	−1.03
SUG4K5	12.45	5.4	1.2	−1.7

Table 1: Description of the different test cases: U_∞ (m/s), Tu_{le} (%), $\Delta x = x_{grid} - x_{le}$ (m).

Zero pressure gradient

The evolution of the intermittency factor γ in function of Re_x for SUG5K0 is shown in figure 3. The experimental values, taken at plateau level, are represented by square boxes. The correspondance of the numerical predicted evolution and the experimental data is very good. Both start, located at Re_x = 93400, and length of transition are well reproduced. In figure 4,

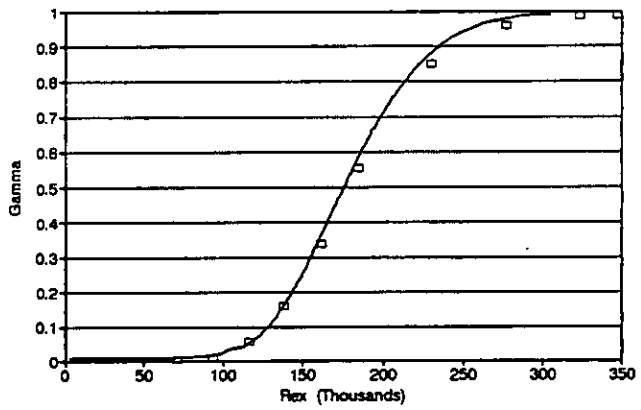

Figure 3: γ-evolution for SUG5K0.

the skin friction C_f, the shape factor H and the momentum thickness θ are given. No experimental values of C_f are available. The analytical laminar and turbulent skin friction coefficient are also plotted in the figure. The experimental evolution of the shape factor starts already to deviate from the laminar value 2.59 upstream of start of transition. Through diffusion of turbulent eddies from the main flow towards the wall, the outer region of the boundary layer is affected firstly. As a consequence, the velocity profile in the outer region tends to a turbulent one through the presence of turhulent Reynolds-stresses. This results in a decrease of the shape factor already upstream of the start of transition. This diffusion should be taken into account in the modelling by defining a normal γ-distribution. This has not

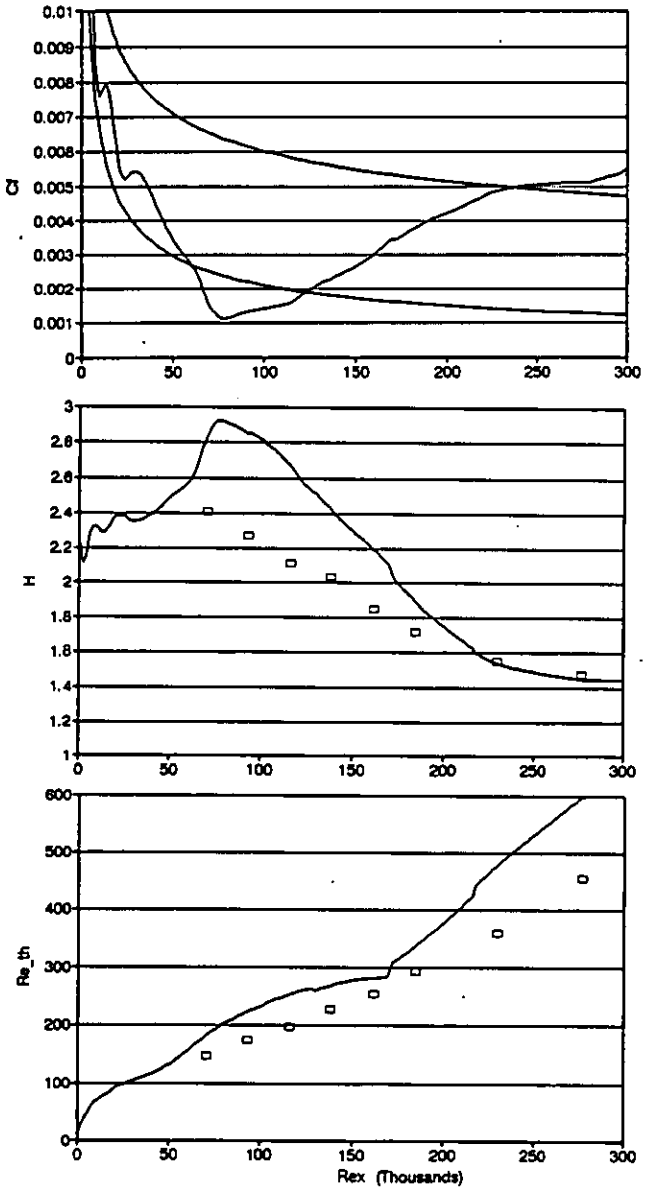

Figure 4: Skin friction coefficient (top), shape factor (middle) and momentum thickness (bottom) for SUG5K0.

yet been introduced in the model. On the leading edge, both the skin friction and the shape factor show some oscillatory behaviour. This can be attributed to irregularities in the geometrical discretization of the leading edge. We preferred to leave these irregularities in the calculations rather than to smooth them because results are very sensitive to details in the shape. Velocity profiles are shown in figure 5. The globally averaged velocity profiles are obtained by weighting the laminar and turbulent conditioned values. Although the mea-

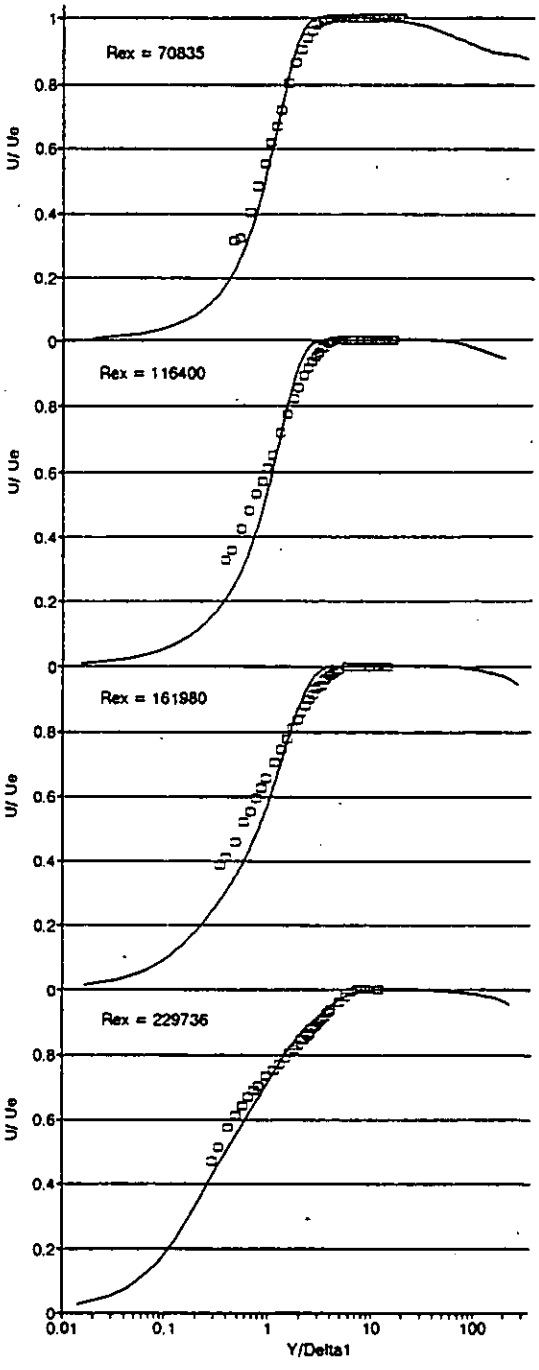

Figure 5: Velocity profiles for different positions on the plate for SUG5K0.

surements have been stopped once a plateau-region was reached, the calculations show that the velocity diminishes further away from the wall. This effect becomes smaller further downstream. The correspondance with the experiments is very good. The profiles of the tur-

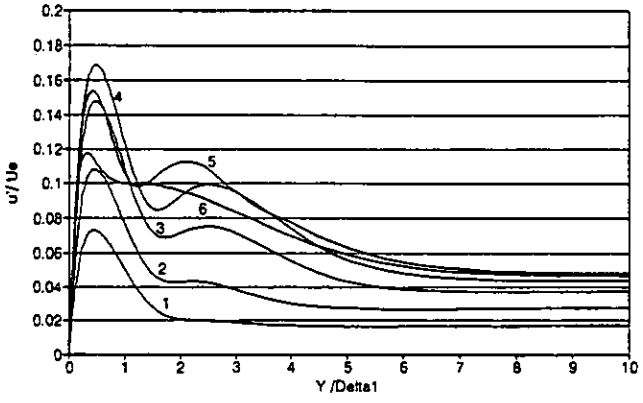

Figure 6: Turbulence intensity profiles for different positions on the plate for SUG5K0.

bulence intensity are given in figure 6. The Tu-level reaches a peak of 17% near the wall midway the transition zone. Only the computed profiles are shown as no experimental data are available. The positions 1 to 6 correspond with the following Re-numbers: 1: 116400; 2: 138300; 3: 162000; 4: 184700; 5: 229700; 6: 267800. We obtain here turbulence levels comparable to these in previous work (Steelant and Dick, 1995) for ZPG flows. So we are confident that also for the present test case, turbulence levels are predicted well although we cannot strictly verify this.

Adverse pressure gradient

The corresponding velocity distributions for the APG-cases are given in figure 7. The evolution of the in-

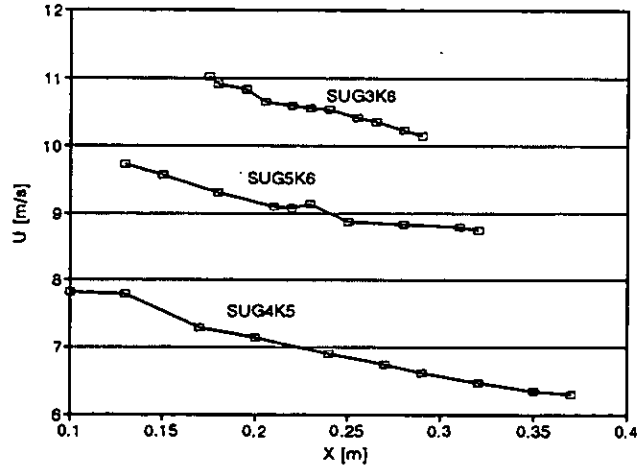

Figure 7: Velocity distribution along the flat plate for SUG5K6, SUG3K6 and SUG4K5.

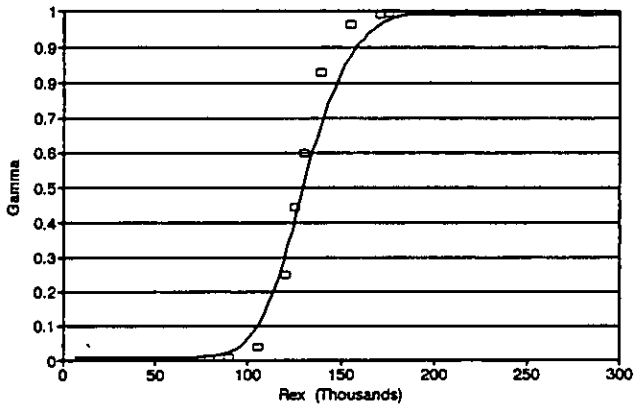

Figure 8: γ-evolution for SUG5K6.

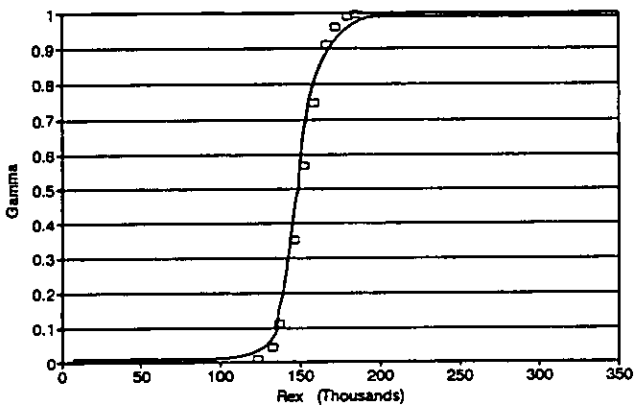

Figure 9: γ-evolution for SUG3K6.

termittency factor γ for SUG5K6 is shown in figure 8. The correspondance of the numerically predicted evolution and the experimental data is very good. The test cases SUG3K6 and SUG4K5 correspond with different turbulence levels and accelaration parameters than the previous test cases, so that a good verification of the proposed correlations for $\widehat{n}\sigma$ can be obtained. Also for this cases, the γ-profiles correspond well with the experimental data (Fig. 9 and 10). For these three test cases, the starts of transition are respectively $Re_z = 90000, 123000, 63450$.

Figure 11 gives the skin friction C_f, the shape factor H and the momentum thickness θ for SUG5K6. Due to the adverse pressure gradient and the high turbulence level, a larger discrepancy is present for the shape factor than in the previous cases. Both the pressure gradient and the turbulence intensity enhance the diffusion of the turbulence towards the wall. Globally, the momentum thickness has the same behaviour as in the measure-

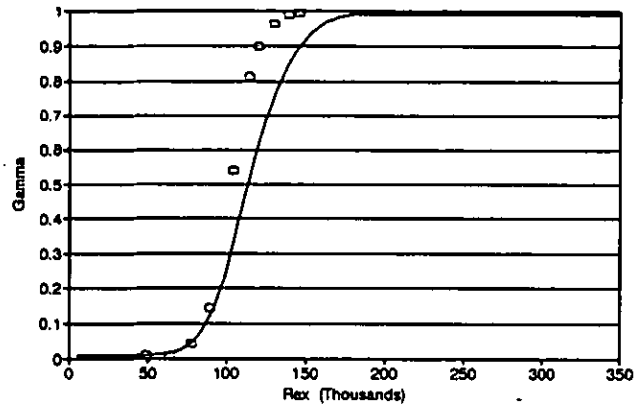

Figure 10: γ-evolution for SUG4K5.

ments. As no experimental data are available, the distributions of the streamwise fluctuations are not given. The numerical results reveal peak values of turbulence level of 25% and higher. Although we cannot make a comparison with experimental data, the obtained levels seem realistic. Velocity profiles, shown in figure 12, correspond reasonably well with the data. The evolution of C_f, the shape factor H and Re_θ for the test cases SUG3K6 and SUG4K5 have a similar behaviour as the previous test cases and are not shown here.

CONCLUSIONS

By the use of conditionally averaged Navier-Stokes equations and a dynamically determined intermittency factor, a very good prediction of bypass transition is obtained. The evolution of the velocity profiles and the intermittency factor γ are in good agreement with the measured profiles. The latter is due to the new correlations for $\widehat{n\sigma}$ in adverse pressure gradients. The numerically obtained shape factor overpredicts the experiments in the beginning of the transition region. This could be improved by bringing in a variation of γ in normal direction.

AKNOWLEDGEMENTS

The research reported here was granted under contract 9.0001.91 by the Belgian National Science Foundation (N.F.W.O.) and under contract IUAP/17 as part of the Belgian National Programme on Interuniversity Poles of Attraction, by the Federal Services of Scientific, Technical and Cultural Affairs (D.W.T.C.).

The data necessary for the present research were provided by Prof. J.P. Gostelow.

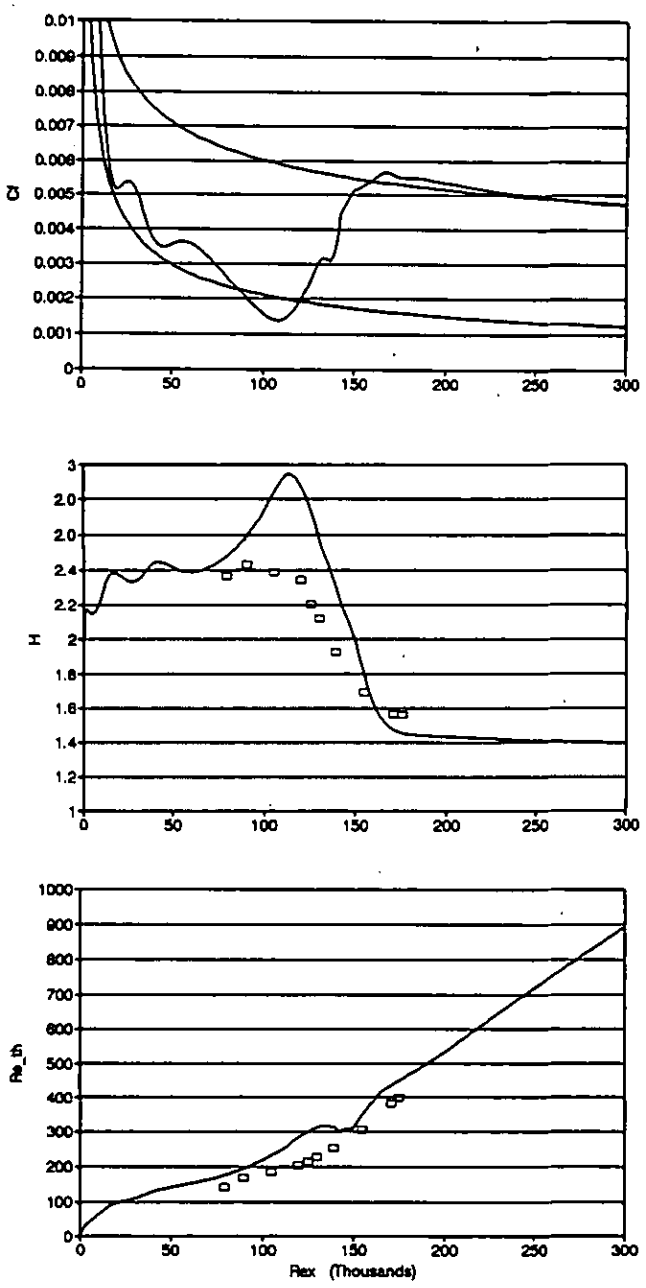

Figure 11: Computed skin friction coefficient together with the analytical laminar and turbulent skin friction (top), shape factor (middle) and momentum thickness θ (bottom) for SUG5K6.

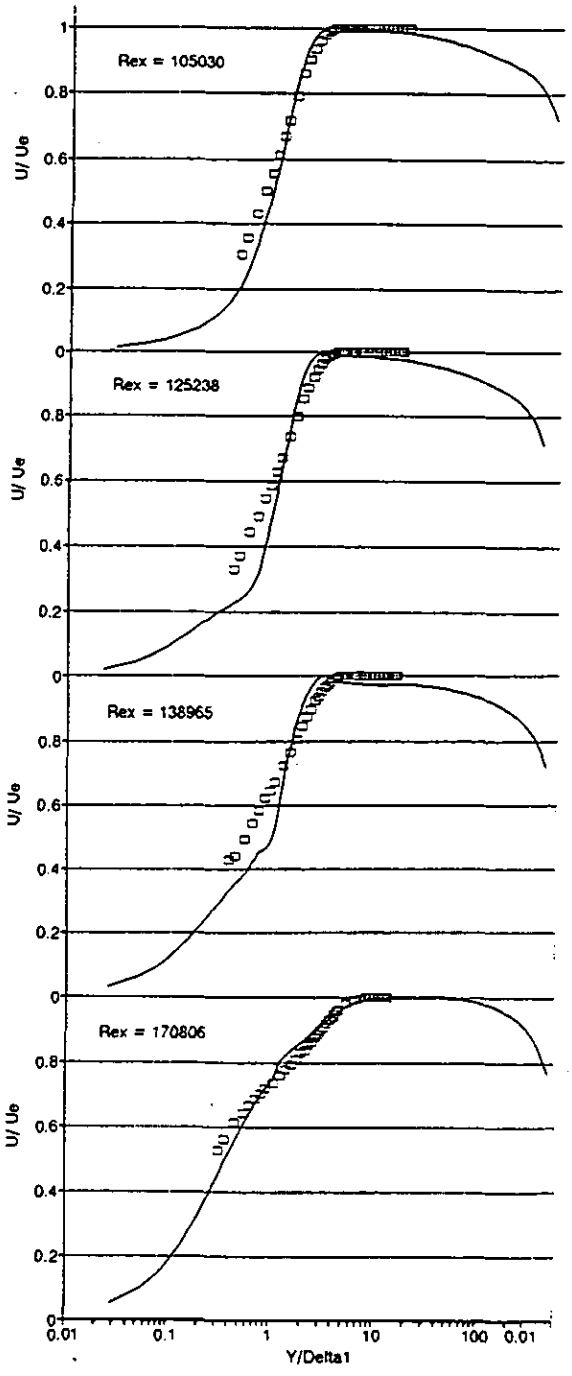

Figure 12: Velocity profiles for different positions on the plate for SUG5K6.

REFERENCES

Blair M.F., 1992, "Boundary-Layer Transition in Accelerating Flows with Intense Freestream Turbulence: Part 2 - The Zone of Intermittent Turbulence", *J. of Turbomachinery*, Vol. 114, pp. 322-332.

Gostelow J.P. and Walker G.J., 1991, "Similarity Behaviour in Transitional Boundary Layers Over a Range of Adverse Pressure Gradients and Turbulence Levels", *J. of Turbomachinery*, Vol. 113, pp. 617-625.

Gostelow J.P., Hong G., Walker G.J. and Dey J., 1994a, "Modeling of Boundary Layer Transition in Turbulent Flows by Linear Combination Integral Method", ASME 94-GT-358.

Gostelow J.P., Blunden A.R. and Walker G.J., 1994b, "Effects of Free-Stream Turbulence and Adverse Pressure Gradients on Bounadry Layer Transition", *J. of Turbomachinery*, Vol. 116, pp. 392-404.

Mayle R., 1991, "The Role of Laminar-Turbulent Transition in Gas Turbine Engines", *J. of Turbomachinery*, Vol. 113, pp. 509-537.

Steelant J. and Dick E., 1994, "A Multigrid Method for the Compressible Navier-Stokes Equations coupled to k -ϵ Turbulence Equations", *Int. J. Num. Methods for Heat and Fluid Flow*, Vol. 4, pp. 99-113.

Steelant J. and Dick E., 1995, "Conditioned Navier-Stokes Equations and $k - \epsilon - \gamma$ Equations to Model Transition in Pressure Gradient Flow", ASME 95-GT-213.

Yang Z. and Shih T.H., 1993, "A New Time Scale k-ϵ Model for Near Wall Turbulence", *AIAA J.* , Vol. 31, pp. 1191-1198.